Photodynamic Therapy

International Edition: DOI: 10.1002/anie.201604130
German Edition: DOI: 10.1002/ange.201604130

# A Mitochondria-Targeted Photosensitizer Showing Improved Photodynamic Therapy Effects Under Hypoxia

*Wen Lv, Zhang Zhang, Kenneth Yin Zhang, Huiran Yang, Shujuan Liu, Aqiang Xu, Song Guo, Qiang Zhao,* and Wei Huang**

***Abstract:*** *Organelle-targeted photosensitizers have been reported to be effective photodynamic therapy (PDT) agents. In this work, we designed and synthesized two iridium(III) complexes that specifically stain the mitochondria and lysosomes of living cells, respectively. Both complexes exhibited long-lived phosphorescence, which is sensitive to oxygen quenching. The photocytotoxicity of the complexes was evaluated under normoxic and hypoxic conditions. The results showed that HeLa cells treated with the mitochondria-targeted complex maintained a slower respiration rate, leading to a higher intracellular oxygen level under hypoxia. As a result, this complex exhibited an improved PDT effect compared to the lysosome-targeted complex, especially under hypoxia conditions, suggestive of a higher practicable potential of mitochondria-targeted PDT agents in cancer therapy.*

Photodynamic therapy (PDT) is an approved photoactivated and non-invasive medical technique that has been widely used for cancer therapy through the generation of excessive reactive oxygen species (ROS).[1] Singlet oxygen ($^1O_2$), as one of the primary toxic ROS, is generated by energy transfer between the triplet excited state of photosensitizers and the ground state of $O_2$.[2] Organelle-targeted PDT agents have been developed and their PDT effect has been studied.[3–5] For example, nucleus-targeted PDT agents caused great damage to cancer cells, but it is not favorable because of the risk of genetic variation.[3] As indispensable organelles, mitochondria and lysosomes play essential roles in cell respiration and digestion, respectively. Importantly, both of them are closely related to cell apoptosis.[6,7] Mitochondria- and lysosome-targeted PDT agents can rapidly damage the biological functions of the organelles under photoactivation, leading to cell death of tumor cells.[4,5] However, investigation was performed under normoxia conditions where oxygen supply was sufficient, which is opposite to the hypoxic solid tumor cells. To develop highly effective organelle-targeted PDT drugs, it is urgent and important to evaluate the relation between organelle-targeting and PDT effect, especially under hypoxia conditions.

In this work, two photosensitizers based on iridium(III) complexes (Ir-P(ph)$_3$ and Ir-alkyl, Scheme 1a,b) were designed and synthesized, which specifically targeted the mitochondria and lysosomes (Scheme 1c), respectively. The complexes exhibited similar photophysical properties and singlet oxygen quantum yields ($\Phi_\Delta$) owing to the same cyclometallating ligands. As the oxygen concentration could greatly influence the PDT effect,[8] imaging experiments of

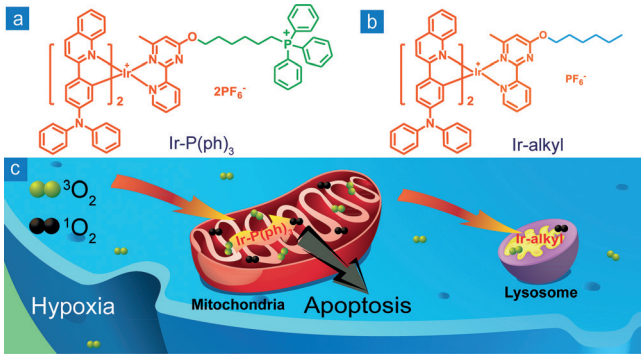


***Scheme 1.*** Chemical structures of a) Ir-P(ph)$_3$ and b) Ir-alkyl, and c) the process of mitochondria- or lysosome-targeted PDT.

HeLa cells treated with the complexes under different oxygen concentrations were conducted. Interestingly, the cells stained with Ir-P(ph)$_3$ maintained a relatively high intracellular oxygen concentration (ic$O_2$) under hypoxic conditions compared to the cells loaded with Ir-alkyl, which probably resulted from respiration inhibition induced by mitochondria-targeted Ir-P(ph)$_3$. The PDT effects of both complexes were evaluated, and the results indicated that the mitochondria-targeted agent was more practicable in cancer therapy.

The synthetic routes of the complexes are shown in the Supporting Information (Scheme S1). The complexes exhibited strong absorption bands located at 380–520 nm, which could be assigned to singlet and triplet metal-to-ligand charge transfer and ligand-to-ligand charge transfer absorption (Figure S1). The emission peaks of Ir-P(ph)$_3$ and Ir-alkyl were located at 590 nm and 600 nm, respectively (Figure S2). Upon

[*] W. Lv, Z. Zhang, Dr. K. Y. Zhang, H. Yang, Prof. S. Liu, A. Xu, S. Guo, Prof. Q. Zhao, Prof. W. Huang
Key Laboratory for Organic Electronics and Information Displays and Institute of Advanced Materials (IAM)
Jiangsu National Synergetic Innovation Center for Advanced Materials (SICAM)
Nanjing University of Posts and Telecommunications (NUPT)
Nanjing 210023 (P.R. China)
E-mail: iamqzhao@njupt.edu.cn
wei-huang@njtech.edu.cn
Prof. W. Huang
Key Laboratory of Flexible Electronics (KLOFE) and Institute of Advanced Materials (IAM)
Jiangsu National Synergetic Innovation Center for Advanced Materials (SICAM)
Nanjing Tech University (NanjingTech)
Nanjing 211816 (P.R. China)

Supporting information for this article can be found under: http://dx.doi.org/10.1002/anie.201604130.

  

increasing oxygen concentration, their luminescence intensity decreased and lifetimes shortened (Figure S2, Table S1). The Stern–Volmer plots revealed a good linear relation (Figure S3).[9] The luminescent quantum efficiencies of Ir-P(ph)$_3$ and Ir-alkyl were 0.13 and 0.15 in water, respectively (Table S2). The singlet oxygen quantum yields of Ir-P(ph)$_3$ and Ir-alkyl were calculated to be 0.17 and 0.21 using methylene blue (MB; $\Phi_\Delta = 0.52$ in DMF) as a standard.[4a,10] The luminescence spectra (Figure S4) and phosphorescence lifetimes (Figure S5) of the complexes in phosphate buffered solution at different pH values remained largely unchanged, indicating that the complexes are not pH dependent. Both Ir-P(ph)$_3$ and Ir-alkyl exhibited long emission lifetime (Table S1) and excellent $O_2$ sensitivity. These results indicated their promising applications as oxygen probes and PDT photosensitizers.

The cell viability was measured through the methyl thiazolyltetrazolium (MTT) assay. HeLa cells were incubated with different concentrations of the complexes in the dark for 24 h. The cell viability remained high, indicating the low dark cytotoxicity of Ir-P(ph)$_3$ and Ir-alkyl (Figure S6). Subsequently, colocalization experiments involving Mito-Tracker Green (MTG) and LysoGreen were conducted to confirm the intracellular distribution of the complexes. The results showed that Ir-P(ph)$_3$ specifically localized in the mitochondria of the cells, while Ir-alkyl was concentrated in the lysosomes (Figure S7, S8). The Pearson's colocalization coefficients of Ir-P(ph)$_3$ with MTG and Ir-alkyl with LysoGreen were 0.85 and 0.91, respectively. Specific mitochondria and lysosome staining was further confirmed using other cell lines, including A549 cells and HepG2 cells (Figure S9–S12).

To evaluate the photostability of the two complexes, photobleaching experiments in living cells were conducted. After strong 488 nm light irradiation, the luminescence intensity of Ir-P(ph)$_3$ and Ir-alkyl were slightly decreased (Figure S13 a, S14 a). In contrast, the luminescence of MTG and LysoGreen was almost completely quenched (Figure S13 b, S14 b), demonstrating the higher photostability of the two complexes than the commercial dyes. The cellular uptake mechanism of Ir-P(ph)$_3$ and Ir-alkyl was investigated by incubating cells with the complexes under different conditions.[11] Compared with cells incubated at 37 °C, the luminescence intensity of cells incubated at 4 °C or pretreated with metabolic inhibitors (deoxy-D-glucose and oligomycin) and endocytosis inhibitors ($NH_4Cl$) was much weaker (Figure S15), indicating that the cellular uptake mechanism of the complexes was energy-dependent endocytosis.

The generation of singlet oxygen depends on the presence of molecular oxygen, which is often inadequately supplied to solid tumor cells.[12] However, the oxygen concentrations in various organelles under hypoxia are still unclear. Thus, the intracellular oxygen concentration of living cells was first determined using confocal microscopy imaging and phosphorescence lifetime imaging (PLIM).[13] A calibration curve for $icO_2$ was constructed using fixed cells because they provided a similar biological environment to living cells and the $icO_2$ in the fixed cells was supposed to be the same as that in the extracellular environment. As shown in Figure S16–S19 and Figure 1 a,b, the fixed HeLa cells loaded with the

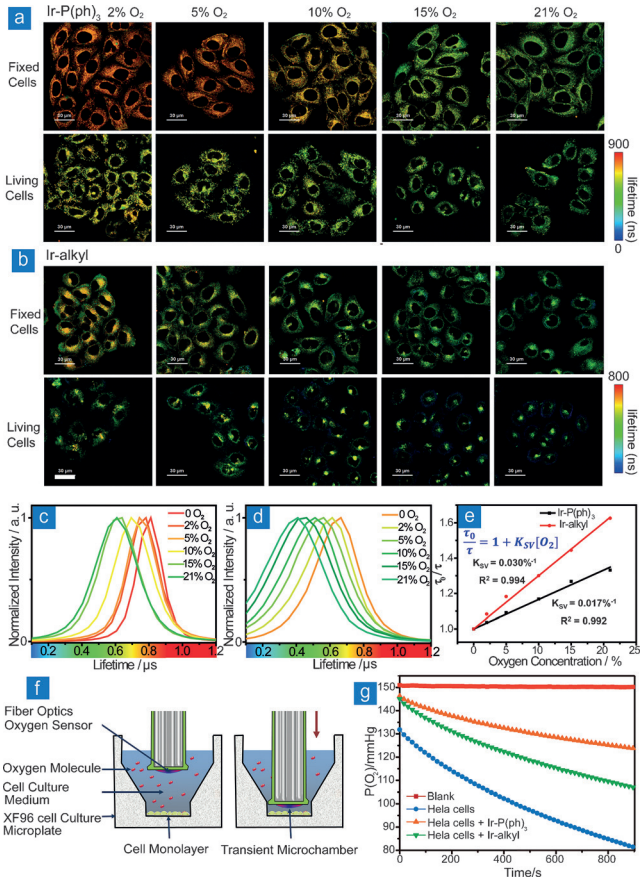


***Figure 1.*** PLIM images of a) Ir-P(ph)$_3$- and b) Ir-alkyl-loaded fixed and living HeLa cells. Luminescence lifetime distributions of PLIM imaging of c) Ir-P(ph)$_3$- and d) Ir-alkyl-treated fixed cells, and e) the fitted Stern–Volmer plots. The cells were incubated with the complexes (5 μM) at 37 °C for 12 h. The images were taken under different oxygen partial pressures. $\lambda_{ex} = 405$ nm, $f = 0.5$ MHz. All of the images share the same scale bar of 30 μm. Images were taken at 37 °C. f) Scheme of the setup to measure the partial pressure of oxygen in cell culture medium. g) The partial pressure of oxygen in cell culture medium under different conditions. The cells were seeded on a 96-well plate at 37 °C for 24 h and then treated with the complexes (5 μM) at 37 °C for 12 h.

complexes displayed enhanced luminescence with elongated lifetimes upon decreasing the extracellular oxygen concentration from 21 % to 2 %, corresponding to a decrease of $icO_2$ from 21 % to 2 %. The calibration curves were fitted through the luminescence lifetime distributions of the PLIM imagings of Ir-P(ph)$_3$- and Ir-alkyl-treated fixed cells under different oxygen concentrations (Figure 1 c–e). According to the calibration curves, the $icO_2$ of the living cells treated with the complexes was determined (Table S3). Under ambient conditions, the living cells treated with Ir-P(ph)$_3$ exhibited a luminescence lifetime of about 562 ns and the mitochondrial oxygen concentration was about 26 %. When the extracellular oxygen concentration was reduced to 2 %, the luminescence lifetime was elongated to 682 ns and the mitochondrial oxygen concentration was calculated to be 11 %. Similarly, the lysosomal oxygen concentration determined according to the microscopy images of living cells treated with Ir-alkyl was calculated to be 3 % when the cells were cultured under 2 %

$O_2$ extracellular conditions. The higher oxygen concentration in mitochondria than in lysosomes is likely the result of cellular respiration. The following experiment was performed to compare the respiration rate of the cells treated with Ir-P(ph)$_3$ and Ir-alkyl. As illustrated in Figure 1 f, cells were cultured in a closed microchamber and the oxygen partial pressure $P_{O2}$ in the culture medium was measured via XF96 Analyzer (Seahorse Bioscience).[14] A lower $P_{O_2}$ value indicated more oxygen consumption and thus a faster respiration rate. Living cells cultured in the microchamber for about 15 min resulted in a decrease of oxygen content by 44% owing to the regulated respiration. When the cells were pretreated with the complexes, the decrease of oxygen content in the culture medium became 18% and 29% for Ir-P(ph)$_3$ and Ir-alkyl, respectively, indicative of a slowed respiration rate (Figure 1 g and Figure S20). Ir-P(ph)$_3$ exhibited a more effective inhibition of mitochondrial respiration than Ir-alkyl, which led to a higher mitochondrial oxygen concentration than the extracellular environment and thus a good PDT performance in hypoxic tumor cells.

The oxygen concentration inside the solid tumors is usually as low as 4%,[12] which seriously limits the PDT effect. As treatment with Ir-P(ph)$_3$ led to a relatively higher oxygen concentrations in the mitochondria, the PDT performance of the complex was tested under hypoxic conditions. Annexin V-FITC and PI were used as the indicators for apoptotic and dead cells, respectively. Cells undergoing early apoptosis would be stained with green luminescent Annexin V-FITC on cell membrane, while further staining with red luminescent PI in the nucleus indicated the apoptosis and cell death. HeLa cells treated with the complexes in the dark remained healthy (Figure S21). Irradiation at 475 nm (22 mW cm$^{-2}$) under normoxia for 30 min led to cell death in 4 h (Figure 2 a).[15] When the cells were cultured under hypoxia conditions (5% $O_2$), light irradiation of the Ir-P(ph)$_3$-treated cells caused cell death in 4 h, while the PDT effect of Ir-alkyl was less efficient (Figure 2 b), which may be due to the relatively high oxygen concentration in mitochondria compared to that in lysosomes and extracellular environments.

The PDT effect of the complexes was further studied using flow cytometry. Increasing the dose concentration or irradiation time led to a higher percentage of dead cells (Figure S22,S23). As expected, irradiation under normoxia brought about a higher percentage of dead cells compared to irradiation under hypoxia (Figure 2 c–f), owing to the sufficient $O_2$ supply. Interestingly, 3.0% dead cells were detected after treatment of the cells with Ir-P(ph)$_3$ (5 μM) for 12 h followed by irradiation at 475 nm under hypoxia for 15 min and then cultured under ambient conditions for 30 min (Figure 2 e), while the percentage was reduced to 0.15% when Ir-alkyl was used (Figure 2 f). This result indicated an improved PDT effect of the mitochondria-targeted Ir-P(ph)$_3$ compared to the lysosome-specific Ir-alkyl under hypoxia.

To confirm that cell death was induced by the photodynamic generation of singlet oxygen, the production of intracellular ROS was investigated. 2′,7′-Dichlorofluorescein-diacetate (DCFH-DA) was used as an indicator, which was converted to green-fluorescent DCF in the presence of ROS. HeLa cells loaded with DCFH-DA followed by 475 nm

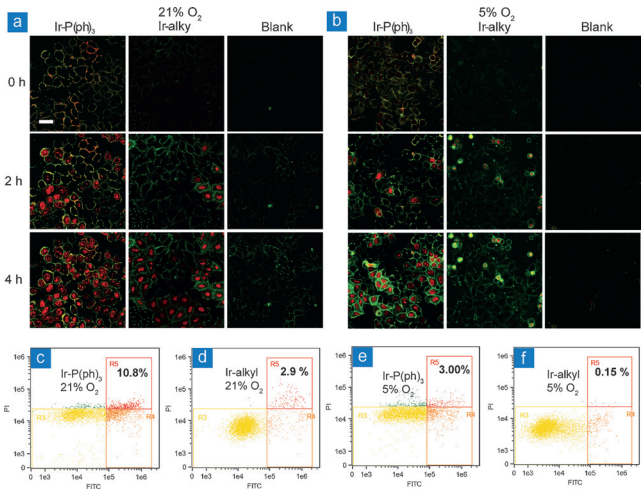


***Figure 2.*** Confocal microscopy images and flow cytometry quantification of annexin V-FITC- and PI-labeled HeLa cells. The cells were treated with the complexes (5 μM) at 37 °C for 12 h. The cells were then incubated under a,c,d) 21% $O_2$ or b,e,f) 5% $O_2$ and irradiated by 475 nm light (22 mW cm$^{-2}$) with a xenon lamp for a,b) 30 min or c–f) 15 min. Cells were viewed in the green channel for annexin V-FITC ($\lambda_{ex}$ = 488 nm, $\lambda_{em}$ = 500–560 nm) and red channel for PI ($\lambda_{ex}$ = 488 nm, $\lambda_{em}$ = 600–680 nm), respectively. The images were taken 0, 2, and 4 h after the irradiation. All the images share the same scale bar of 50 μm. Images were taken at 25 °C.

irradiation (22 mW cm$^{-2}$) displayed dim green fluorescence as revealed in the confocal microscopy images (Figure S24). When the cells were pretreated with the complexes, intense green fluorescence was observed, indicating the generation of intracellular ROS (Figure S25, S26). The luminescence intensity of DCF in the Ir-P(ph)$_3$-treated cells was stronger than that of Ir-alkyl-treated cells, indicative of more ROS production. These cells were analyzed by flow cytometry. When Ir-P(ph)$_3$-treated cells were irradiated under normoxia, 80% of the cells exhibited intense DCF fluorescence (Figure S27 a). When the irradiation was performed under hypoxia, 63% cells were green-emissive (Figure S28a). When Ir-alkyl was used, irradiation under normoxia and hypoxia resulted in 35% and 14% cells, respectively, exhibiting green fluorescence (Figure S27b, S28b). Again, the photodynamic ROS generation was more efficient in the cells treated with the mitochondria-targeted Ir-P(ph)$_3$ compared to those loaded with the lysosome-specific Ir-alkyl.

Since early apoptotic cells undergo characteristic depolarization of the mitochondria,[16] the mitochondrial membrane potentials (MMP) were measured using JC-1 as an indicator, which was converted from aggregation state to monomer upon decreasing MMP accompanied with a fluorescence color change from red to green. In a positive control experiment, carbonyl cyanide *m*-chlorophenyl hydrazone (CCCP) was used to induce the decrease of MMP. HeLa cells treated with JC-1 exhibited red and green fluorescence. Pretreatment with CCCP caused quenching of the red fluorescence and enhancement of the green fluorescence (Figure S29). Similar MMP decreasing has also been observed when the cells were treated with the mitochontria-targeted Ir-P(ph)$_3$ followed by 475 nm irradiation (22 mW cm$^{-2}$) under

  

normoxia and hypoxia (Figure S30a,S31a). In contrast, the cells treated with the lysosome-targeted Ir-alkyl did not exhibit MMP decreasing (Figure S30b,S31b).

The PDT effect of the complexes under normoxia and hypoxia was evaluated by the MTT assay. The cells incubated with Ir-P(ph)$_3$ for 12 h maintained 87% cell viability, which dramatically decreased to 7.6% right after light irradiation, and further to 2.3% in 4 h under normoxia. When the irradiation was performed under hypoxia, 3.3% cell viability was obtained in 4 h (Figure 3a), indicating a high PDT

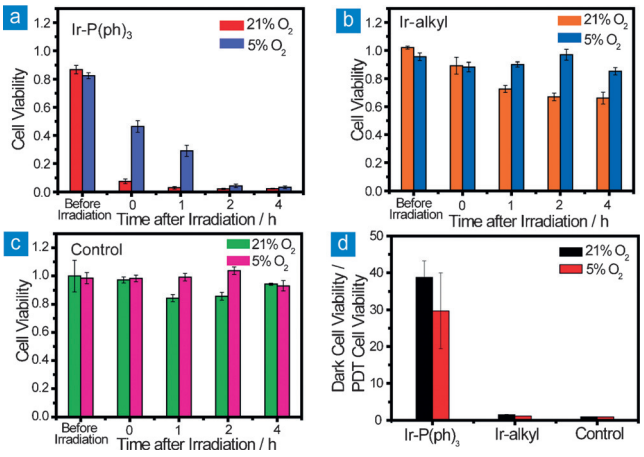


***Figure 3.*** In vitro cell viability of HeLa cells. The cells were incubated with a) Ir-P(ph)$_3$ (5 μM), b) Ir-alkyl (5 μM), and c) DMSO (2.5%) at 37°C for 12 h and then incubated under 21% and 5% $O_2$. The cells were then irradiated by 475 nm light (22 mW cm$^{-2}$) with a xenon lamp for 30 min. The cell viability was measured 0, 1, 2, and 4 h after the irradiation. d) The ratio of dark cell viability to PDT cell viability.

efficiency. In contrast, the cell viability of Ir-alkyl-loaded and untreated cells remained at a high percentage (>66%) under hypoxic or normoxic conditions (Figure 3b,c). The viability ratio of the cells without and with light irradiation is summarized in Figure 3d. The Ir-P(ph)$_3$-treated cells showed viability ratios of 39 and 30 under normoxia and hypoxia, respectively. For the Ir-alkyl-loaded and untreated cells, the ratio was below 1.5. These results indicated a good PDT effect of the mitochondria-targeted complex Ir-P(ph)$_3$ under hypoxia, which was more practical in the therapy of hypoxic solid tumors.

In summary, we have developed two iridium(III) complexes to evaluate the PDT effect of mitochondria- and lysosome-targeted photosensitizers under normoxic and hypoxic conditions. Our results showed that the mitochondria-targeted PDT agent exhibited improved therapeutic effects compared to the lysosome-targeted agent. One possible explanation is that the mitochondria-targeted photosensitizer inhibited mitochondrial respiration, resulting in higher intramitochondrial oxygen content, especially under hypoxia conditions, which is advantageous for PDT in hypoxic tumor cells. We think that this work is meaningful for designing and developing high effective organelle-targeted PDT agents, which has great potential in biomedical fields.

## Acknowledgements

This work was supported by National Natural Science Foundation of China (51473078, 61136003), National Program for Support of Top-Notch Young Professionals, Scientific and Technological Innovation Teams of Colleges and Universities in Jiangsu Province (TJ215006), Natural Science Foundation of Jiangsu Province of China (BK20130038, BM2012010), Synergetic Innovation Center for Organic Electronics and Information Displays and Priority Academic Program Development of Jiangsu Higher Education Institutions (YX03001).

**Keywords:** cell death · hypoxia · iridium · photodynamic therapy · singlet oxygen

**How to cite:** *Angew. Chem. Int. Ed.* **2016**, *55*, 9947–9951
*Angew. Chem.* **2016**, *128*, 10101–10105

[1] C. Mari, V. Pierroz, S. Ferrari, G. Gasser, *Chem. Sci.* **2015**, *6*, 2660–2686.
[2] a) J. P. Celli, B. Q. Spring, I. Rizvi, C. L. Evans, K. S. Samkoe, S. Verma, B. W. Pogue, T. Hasan, *Chem. Rev.* **2010**, *110*, 2795–2838; b) N. J. Farrer, L. Salassa, P. J. Sadler, *Dalton Trans.* **2009**, 10690–10701; c) R. Lincoln, L. Kohler, S. Monro, H. M. Yin, M. Stephenson, R. F. Zong, A. Chouai, C. Dorsey, R. Hennigar, R. P. Thummel, S. A. McFarland, *J. Am. Chem. Soc.* **2013**, *135*, 17161–17175; d) J. D. Knoll, C. Turro, *Coord. Chem. Rev.* **2015**, *282*, 110–126; e) B. S. Howerton, D. K. Heidary, E. C. Glazer, *J. Am. Chem. Soc.* **2012**, *134*, 8324–8327; f) B. A. Albani, B. Pena, N. A. Leed, N. A. B. G. de Paula, C. Pavani, M. S. Baptista, K. R. Dunbar, C. Turro, *J. Am. Chem. Soc.* **2014**, *136*, 17095–17101; g) C. Mari, V. Pierroz, R. Rubbiani, M. Patra, J. Hess, B. Spingler, L. Oehninger, J. Schur, I. Ott, L. Salassa, S. Ferrari, G. Gasser, *Chem. Eur. J.* **2014**, *20*, 14421–14436; h) S. L. H. Higgins, K. J. Brewer, *Angew. Chem. Int. Ed.* **2012**, *51*, 11420–11422; *Angew. Chem.* **2012**, *124*, 11584–11586; i) L. M. Loftus, J. K. White, B. A. Albani, L. Kohler, J. J. Kodanko, R. P. Thummel, K. R. Dunbar, C. Turro, *Chem. Eur. J.* **2016**, *22*, 3704–3708; j) S. Bhattacharyya, I. Chakraborty, B. K. Dirghangi, A. Chakravoty, *Inorg. Chem.* **2001**, *40*, 286–293.
[3] J. Bertram, *Mol. Aspects Med.* **2000**, *21*, 167–223.
[4] a) Y. Li, C. Tan, W. Zhang, L. He, L. Ji, Z. Mao, *Biomaterials* **2015**, *36*, 95–104; b) K. Han, Q. Lei, S. Wang, J. Hu, W. Qiu, J. Zhu, W. Yin, X. Luo, X. Zhang, *Adv. Funct. Mater.* **2015**, *25*, 2961–2971; c) S. P. Y. Li, C. T. S. Lau, M. W. Louie, Y. W. Lam, S. H. Cheng, K. K. W. Lo, *Biomaterials* **2013**, *34*, 7519–7532.
[5] H. Huang, B. Yu, P. Zhang, J. Huang, Y. Chen, G. Gasser, L. Ji, H. Chao, *Angew. Chem. Int. Ed.* **2015**, *54*, 14049–14052; *Angew. Chem.* **2015**, *127*, 14255–14258.
[6] S. Fulda, L. Galluzzi, G. Kroemer, *Nat. Rev. Drug Discovery* **2010**, *9*, 447–464.
[7] a) G. Kromer, M. Jaattela, *Nat. Rev. Cancer* **2005**, *5*, 886–897; b) P. Safting, J. Klumperman, *Nat. Rev. Mol. Cell Biol.* **2009**, *10*, 623–635.
[8] a) A. L. Maas, S. L. Carter, E. P. Wileyto, J. Miller, M. Yuan, G. Q. Yu, A. C. Durham, T. M. Busch, *Cancer Res.* **2012**, *72*, 2079–2088; b) Y. Cheng, H. Cheng, C. Jiang, X. Qiu, K. Wang, W. Huan, A. Yuan, J. Wu, Y. Hu, *Nat. Commun.* **2015**, *6*, 8785.
[9] a) D. B. Papkovsky, R. I. Dmitriev, *Chem. Soc. Rev.* **2013**, *42*, 8700–8732; b) X. Wang, O. S. Wolfbeis, *Chem. Soc. Rev.* **2014**, *43*, 3666–3761.
[10] J. Tian, L. Ding, H. Xu, Z. Shen, H. Ju, L. Jia, L. Bao, J. Yu, *J. Am. Chem. Soc.* **2013**, *135*, 18850–18858.

  

[11] S. J. Liu, H. Liang, K. Y. Zhang, Q. Zhao, X. B. Zhou, W. J. Xu, W. Huang, *Chem. Commun.* **2015**, *51*, 7943 – 7946.
[12] W. R. Wilson, M. P. Hay, *Nat. Rev. Cancer* **2011**, *11*, 393 – 410.
[13] W. Lv, T. Yang, Q. Yu, Q. Zhao, K. Y. Zhang, H. Liang, S. Liu, F. Li, W. Huang, *Adv. Sci.* **2015**, *2*, 1500107.
[14] L. Wu, D. Wang, L. Parhamifar, A. Hall, G. Chen, S. M. Moghimi, *Adv. Healthcare Mater.* **2014**, *3*, 817 – 824.
[15] a) S. Moromizato, Y. Hisamatsu, T. Suzuki, Y. Matsuo, R. Abe, S. Aoki, *Inorg. Chem.* **2012**, *51*, 12697 – 12706; b) A. Nakagawa, Y. Hisamatsu, S. Moromizato, M. Kohno, S. Aoki, *Inorg. Chem.* **2014**, *53*, 409 – 422; c) A. Kando, Y. Hisamatsu, H. Ohwada, T. Itoh, S. Moromizato, M. Kohno, S. Aoki, *Inorg. Chem.* **2015**, *54*, 5342 – 5357.
[16] D. R. Green, G. Kroemer, *Science* **2004**, *305*, 626 – 629.

Received: April 28, 2016
Revised: June 8, 2016
Published online: July 6, 2016

  